Communications in Physics, Vol. 35, No. 2 (2025), pp. 181-192
DOI: https://doi.org/10.15625/0868-3166/22113

Broadband metamaterial absorber using multi-disk structure in the THz region

Nguyen The An[1], **Nguyen Thu Minh**[1], **Vu Duy Chien**[1], **Vu Dinh Lam**[3], **Pham Van Hai**[1,2], **Pham Van Dien**[1], **Nguyen Thi Thuy**[1], **Tran Manh Cuong**[1,†]

[1]*Faculty of Physics, Hanoi National University of Education, 136 Xuan Thuy, Cau Giay, Hanoi, Vietnam*

[2]*Institute of Natural Sciences, Hanoi National University of Education, 136 Xuan Thuy, Cau Giay, Hanoi, Vietnam*

[3]*Graduate University of Science and Technology, Vietnam Academy of Science and Technology, 18 Hoang Quoc Viet, Cau Giay, Hanoi, Vietnam*

E-mail: [†]tmcuong0279@gmail.com

Received 26 December 2024
Accepted for publication 12 March 2025
Published 29 May 2025

Abstract. *This study has conducted the design, simulation, and optimization of the broadband metamaterial absorber with a multilayer disk structure which works in the THz region. Through the process of combining various materials and adjusting the correlation parameters between them, the three-layer structure demonstrates a high absorption capability within the frequency range of 5.6-7.9 THz, with an average absorption rate of up to 95%. The analytical results regarding the distribution of electric and magnetic fields on the surface and the electrical equivalent circuit model of the material, further elucidate the absorption principles of the structure. Particularly, this structure also demonstrates an advantage in its ability to function effectively when the angle of incidence is altered up to 45 degrees.*

Keywords: Broadband; multi-layer; multi-disk.

Classification numbers: 41.20.-q; 42.25.Bs; 78.67.Pt.

1. Introduction

Metamaterials (MMs) have numerous practical applications that have been demonstrated across significant frequency ranges from GHz to THz [1–4], including biosensors, absorbers, smart solar energy management, energy harvesting, pressure, density, and volumetric moisture

sensing, as well as cloaking devices [3–6]. Consequently, in recent years, MMs have been extensively researched and have gained greater popularity, from MHz and GHz to THz range. MMs are materials characterized by their magnetic permeability, electrical permittivity, and acoustic refractive index, along with several other unique properties such as acoustic refractive index, subwavelength diffraction, and acoustic Doppler effect. Consequently, MMs have garnered significant interest from the scientific community. Fundamentally, MMs consist of three layers: the first and third layers are composed of metals, while the second layer is an insulating dielectric.

Metamaterial absorber (MMA) is an important branch of MMs and can be categorized into two directions: multi-peak perfect absorbers and broadband absorbers [5–8]. While multi-peak absorbers have been demonstrated to be effective in various applications, the current research focus has shifted towards broadband MMA to develop a wider range of applications such as photovoltaics, stealth technology, and optical waveguides.

In recent years, scientists have focused on various broadband metamaterial absorbers (BMMA) as follows: Horizontally expanded structures have been extensively studied by researchers [9–11]; these structures have achieved wide bandwidths through modifications in structural ratios or the rotation of surface materials. Multilayered MMAs operate differently; typically, each layer functions as a small resonator, generating distinct absorption peaks as demonstrated in previous studies [12–16]. Each small resonator generates absorption peaks at different frequencies based on the variations in the size ratios of the material layers within each resonator. Subsequently, when these small resonators (layers) are stacked, in addition to creating additional absorption peaks to broaden the operational bandwidth, there is also the potential to enhance the absorption level of the preceding resonator. This demonstrates that multilayer structures operate on a clear principle and are effective in generating wide bandwidths.

In this research, the degine, simulation and optimizatiion of a metamaterial absorber structure with broadband capabilities in the terahertz (THz) region exhibiting an average absorption exceeding 90% will be presented. This MMs structure demonstrates an absorption spectrum ranging from 5.6 to 7.9 THz, with high absorption rates above 95% at frequencies of 5.78, 6.8, and 7.6 THz. The lowest absorption region has been optimized to achieve an absorption rate exceeding 79%. The utilization of a multilayer disk structure, with varying disk sizes across the layers, contributes to a high stability of the absorption spectrum even when the angle of incidence increases to 45 degrees. Each disk layer complements one another, resulting in the effective operational capability of the metamaterial and promising numerous applications in the future.

2. Unit Cell Design

Initially, we proceed to design the simplest structure illustrated in Fig. 1, which includes: a Polyimide dielectric layer (with a period of $a = 16\ \mu$m, thickness $h = 0.6\ \mu$m, dielectric constant of $\varepsilon = 3.5$, and electric tangent $\delta = 0.0027$), a gold substrate with dimensions similar to the dielectric layer, differing only in thickness at 0.05 μm. Additionally, a Chromium disk is surrounded by a Gold rim with two radius R and r. We consider the two adjacent material layers, Polyimide and GC (Gold-Chromium), as a single layer for the subsequent study of multilayer structures. The GC metal has a thickness of $d = 0.05\ \mu$m. The complete structure we constructed consists of three layers with varying radii of the GC disk. The size of the disks decreases from bottom to top as shown in Fig. 1c, forming a “pyramidal” structure made of circular disks.

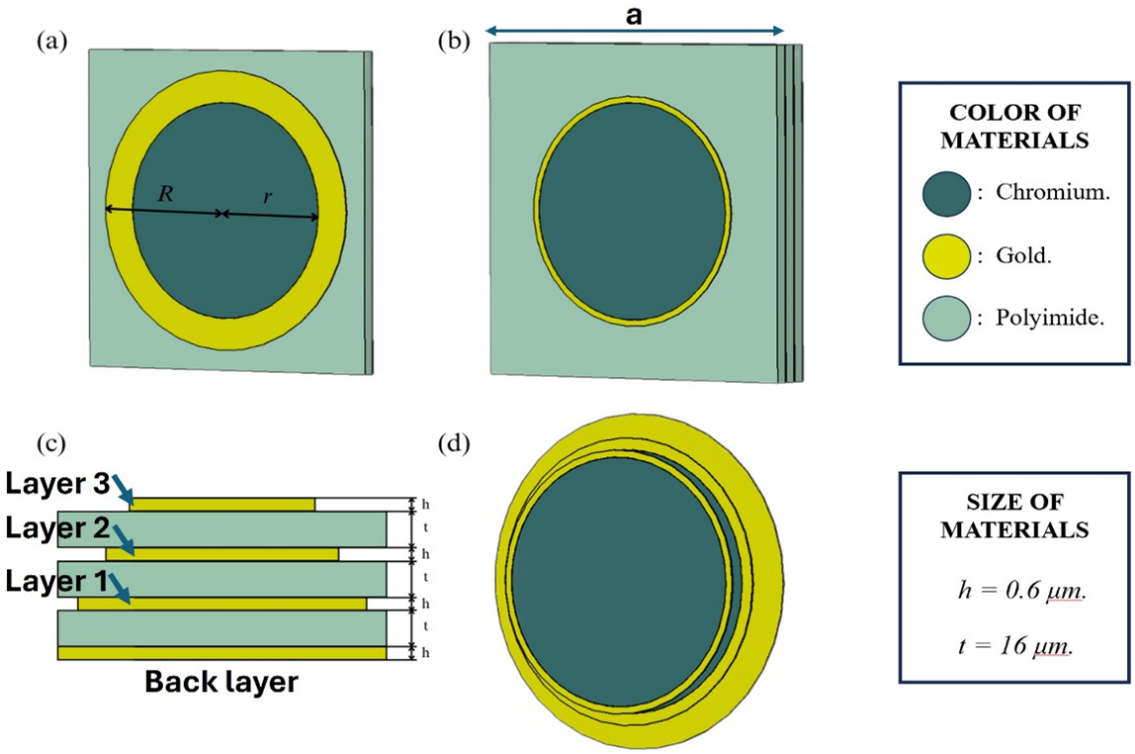

Fig. 1. Perspective view of (a) 1-layer structure, (b) 3-layer structure and side view of (c) 3-layer structure and perspective view of the layered metal part.

The analytical method in this study primarily relies on simulations conducted using CST Microwave Studio®, a robust tool for modeling electromagnetic phenomena. To ensure accuracy in the simulations, we apply periodic electromagnetic boundary conditions, which facilitate the modeling of an unbounded space. This enables us to accurately calculate the electromagnetic density in the vicinity of the MMA structure, thereby reflecting the actual conditions that this structure will encounter in its operational environment.

During the simulation process, we did not consider each material layer as individual components; rather, our objective was to investigate the entire multilayer structure as a unified entity. This approach enables us to assess the interactions between the layers and their impact on the overall electromagnetic absorption performance of the structure. By analyzing the entire structure, we can obtain deeper insights into the operational mechanisms of absorption units, as well as optimize the design to achieve higher absorption efficiency in practical applications. We are able to conduct detailed analyses regarding how factors such as layer thickness, structural ratio, and the materials employed influence electromagnetic absorption capabilities. The results of these analyses will provide a foundation for the development of wideband metamaterial structures with high absorption performance, serving applications in the fields of photovoltaics, solar cells, stealth technology, and advanced optical devices.

3. Results and discussion

3.1. Simulation results of absorptivity, field and current distributions

In this study, starting from a simple structure of 1 layer and progressing to 2 and 3 layers, results have been obtained through simulation as presented in Fig. 2.

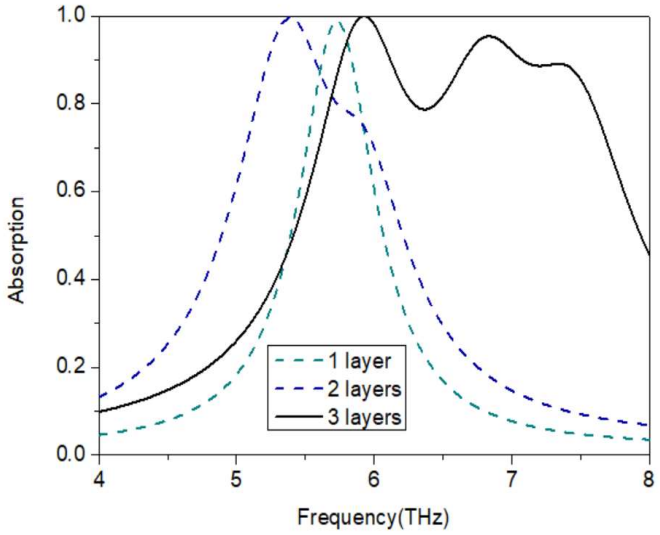

Fig. 2. Simulated absorptivity results for the structures comprising 1, 2, and 3 layers.

In general, through optimization methods with varying dimensions of the structural layers, the obtained absorption spectrum typically manifests as a narrow band and has not been significantly broadened. However, studies have indicated that increasing the number of GC layers can markedly enhance the absorption performance of the structure. Specifically, the incorporation of a third GC layer into the design has been implemented with the expectation of creating a structure with the desired absorption characteristics.

By altering the aspect ratio among the GC layers, the optimal structure with dimensions: $r_1 = 5.4\ \mu$m, $R_1 = 7\ \mu$m, $r_2 = 5.5\ \mu$m, $R_2 = 6\ \mu$m, $r_3 = 5.2\ \mu$m, $R_3 = 5.5\ \mu$m has demonstrated a significant improvement in absorption spectra, exhibiting a broader absorption range and an average absorption exceeding 90% (Fig. 3). This not only indicates the robust absorption capability of the structure but also validates its stability with the ability to operate independently of polarization with an incident angle variation of up to 45 degrees (Fig. 4).

The optimal structure yields a broad absorption spectrum ranging from 5.6 to 7.9 THz, with high absorption rates exceeding 90% at frequencies of 5.78, 6.8, and 7.6 THz, while the lowest absorption region has also been optimized to above 79% (Fig. 3). The pyramidal multilayer-disk structures have the ability to perform well in polarization with incident waves because the incident waves along the z-axis (vertical direction) must traverse multiple layers of material. When the incident angle of the incident wave increases, the components of the electromagnetic vector are still well resonated with the structure and the electromagnetic wave is better confined in the structure, therefore the absorption is not significantly decreased with large incident angles. This

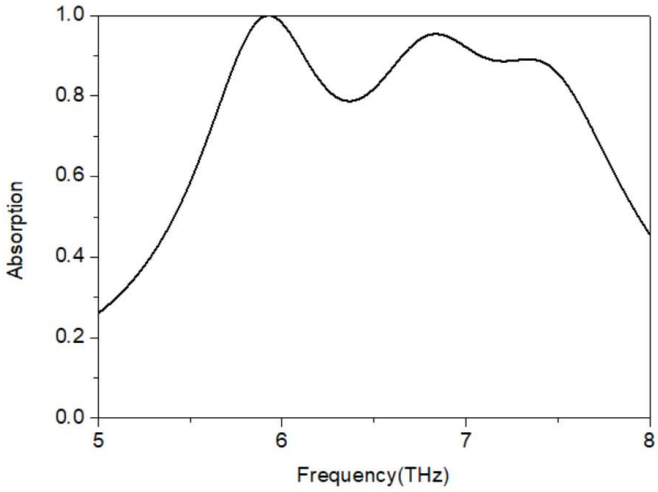

Fig. 3. Simulated absorptivity results for the structures comprising 3 layers.

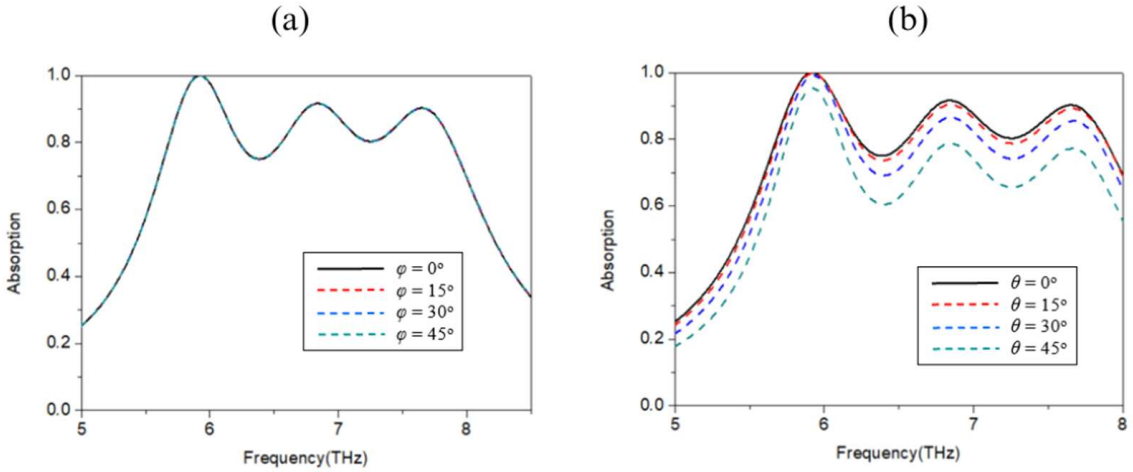

Fig. 4. Absorption spectrum when changing the incident wave angle: (a) changing φ (b) changing θ.

is in contrast to single layer structures. The multilayer structure (3 layers structures) we propose operates effectively with incident angles of up to 45 degrees (Fig. 4).

The investigation of the field distribution on the surface of the material structure not only provides us with deeper insights into the energy distribution but also clarifies the absorption mechanisms of this material. Therefore we conducted this survey on the optimal structure that we have designed (Fig. 5). We compare the distribution of the electric field on the top layer at a high absorption frequency of 7.68 GHz and outside the operational range of the optimal structure, the density of the electromagnetic and magnetic field distribution is primarily concentrated around the

edges of the copper discs. This concentration demonstrates that the GC disks play a crucial role in the electromagnetic absorption capacity of the material.

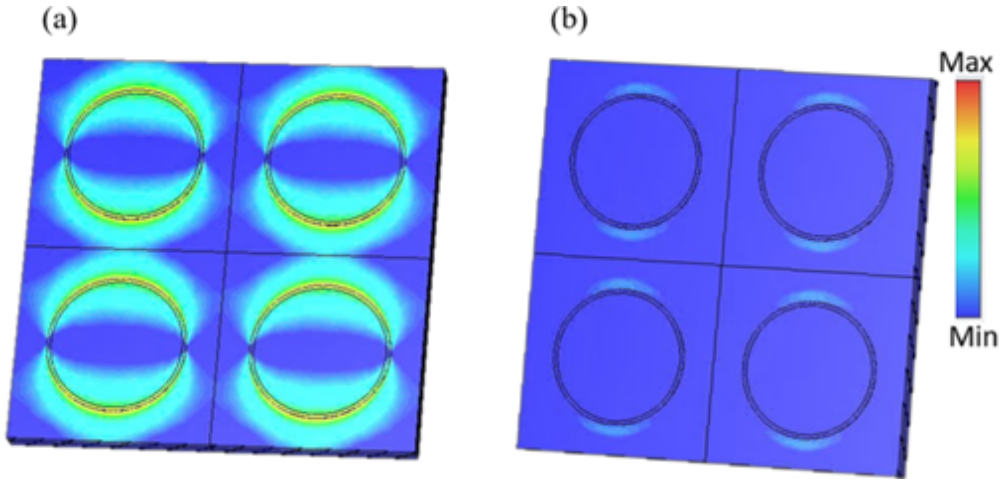

Fig. 5. Simulated electric field and magnetic field density distribution for the broadband absorber at absorption frequencies of (a) 7.68 THz and (b) outside of the active region (normal incident wave).

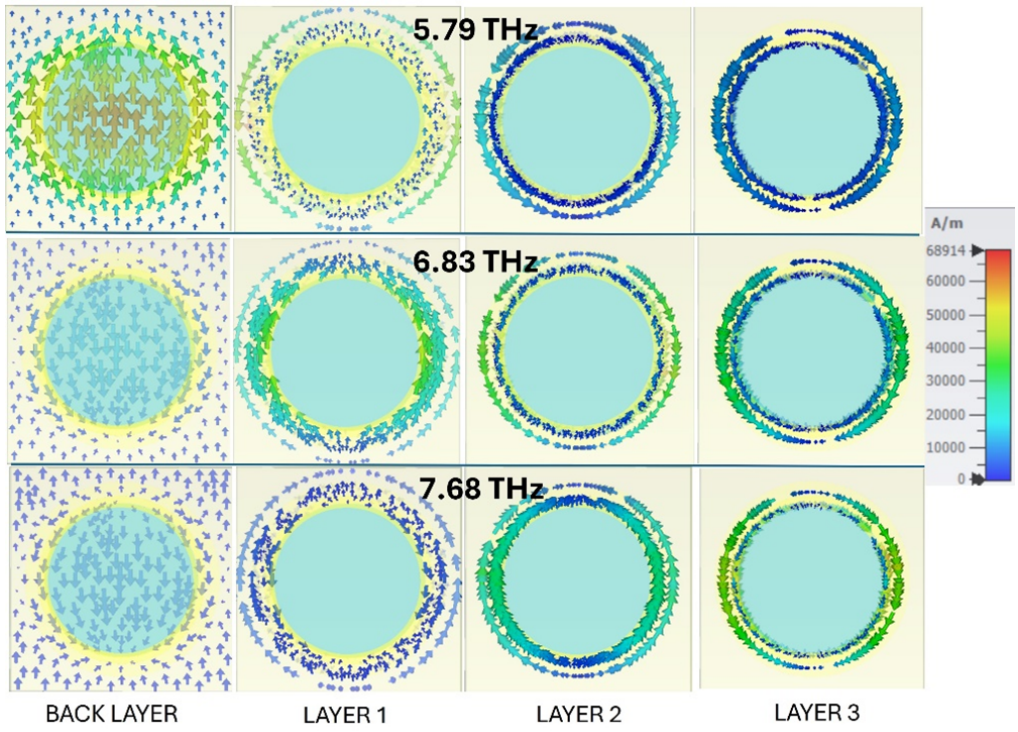

Fig. 6. Surface current of the optimal structure at different frequencies.

In order to clarify the resonance mechanism in the optimal structure, the surface current density is observed through simulation and presented in Fig. 6 (the order of layers is the same in Fig. 1c). It can be clearly seen that most of the resonances occurring on the disks are magnetic resonances when the currents between the disks and the back layer are antiparallel. However, at frequencies of 6.83 THz and 7.68 THz, three corresponding electric resonances are still observed when the currents on the two opposite surfaces are parallel.

3.2. Polarization of incident wave

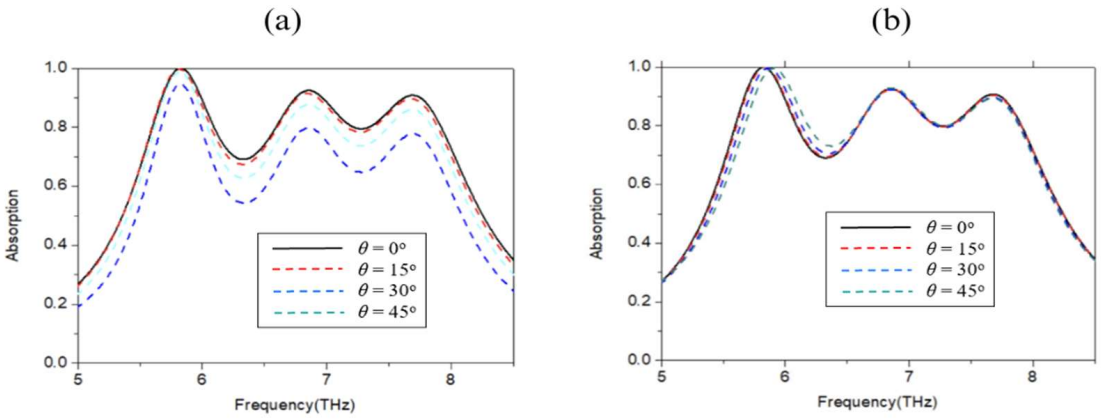

Fig. 7. Angular dependence of the absorption spectrum for the broadband metamaterials absorber: (a) TE mode, (b) TM mode.

Multilayer disk structures have superior ability to maintain stable absorption performance even when the angle of incidence of the waves varies considerably. This mechanism can be explained by the multilayer structure, which compels the incident waves to interact with multiple layers of different materials, thereby minimizing the dependence on the angle of incidence compared to two-dimensional structures, this is also mentioned in the previous section. In our study, the multilayer structure demonstrated effective and stable operation with incidence angles of up to 45 degrees for both TE and TM mode (Fig. 7).

3.3. Circuit Equivalent

Through the distribution of the electromagnetic field and the magnetic field of each structural layer presented in Fig. 8, we observe that each structural layer operates independently of one another, yet they all share a common absorption mechanism. Based on these distributions of the electric field and magnetic field, we have developed an equivalent LC circuit model for each layer of the structure, as illustrated in Fig. 9. It is worth noting that in many metamaterial-based absorber designs, the resistance (R) does not need to be explicitly added because the material itself has intrinsic loss mechanisms. This simplifies the design while still ensuring high absorption efficiency.

The structural layers operate independently of one another; however, they share a common equivalent LC circuit model. To facilitate calculations, we represent the equivalent LC circuit

model of each structural layer in Fig. 10 and compute the corresponding values of inductance (L) and capacitance (C) for each structural layer.

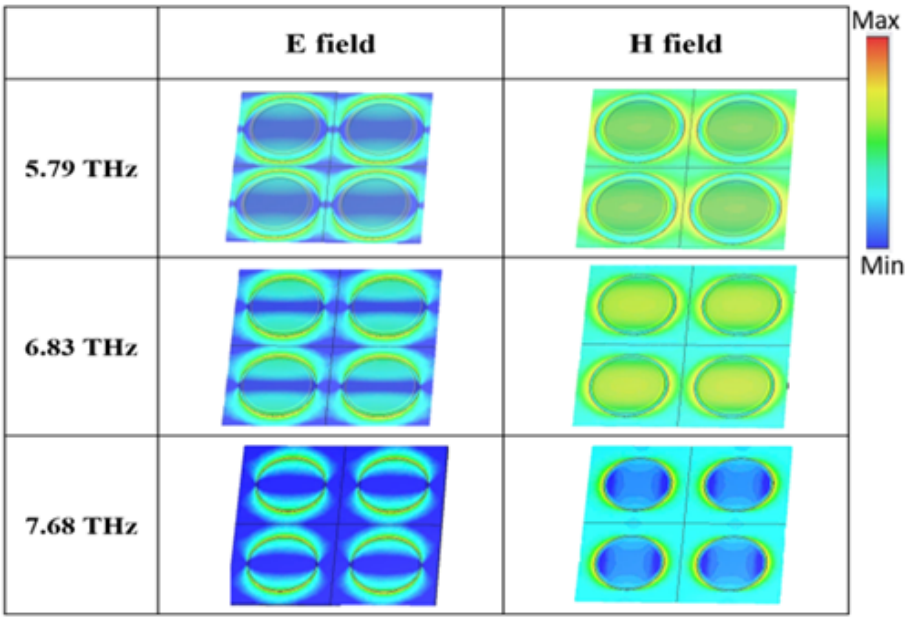

Fig. 8. Simulated electric field and magnetic field distribution for the broadband absorber of first layer structure, second layer structure, third layer structure (from top to bottom).

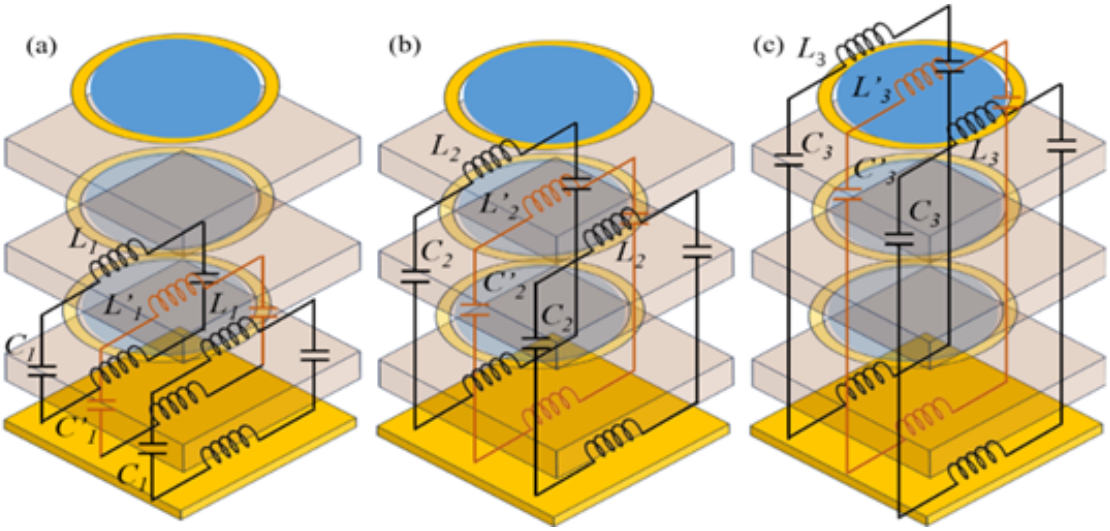

Fig. 9. Equivalent LC circuit model of first layer structure, second layer structure, third layer structure (from left to right).

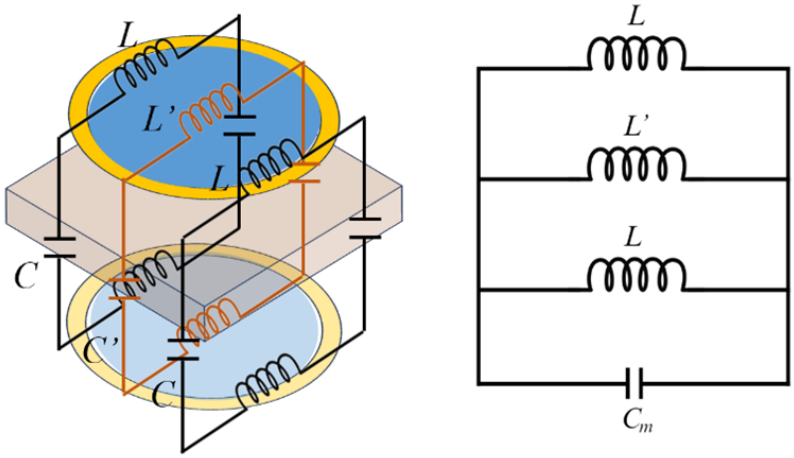

Fig. 10. General equivalent LC circuit model (3D model – left and the circuit model – right).

For circular disk structures or ring-shaped structures, the formula for calculating effective capacitance (C or C') is expressed as follows [17–20]:

$$C = \varepsilon_0 \varepsilon c_1 \frac{\pi(R^2 - r^2)}{t}, \tag{1}$$

where ε_0 is the permittivity of the medium, ε is the permittivity of the dielectric layer and c_1 is a geometrical factor of $0.2 \leq c_1 \leq 0.3$.

From the LC circuit model of each structural layer, the effective capacitance of each structural layer can be calculated using the following formula:

$$C_m = \frac{2C + C'}{3}. \tag{2}$$

From the geometry of ring structure, one can calculate the inductance of ring L and L', as below:

$$\begin{aligned} L &= \int_{-(t+2t_m)/2}^{(t+2t_m)/2} dz \left[\int_{-R}^{-r} \frac{\mu}{2\sqrt{R^2 - y^2}} dy + \int_{-r}^{r} \frac{\mu\sqrt{R^2 - y^2}}{2(R-r)R} dy + \int_{r}^{R} \frac{\mu}{2\sqrt{R^2 - y^2}} dy \right] \\ &= (t + 2t_m)\mu \left[\frac{\pi}{2} - \arcsin\frac{r}{R} + \frac{R}{R-r} \left(\frac{1}{2} \arcsin\frac{r}{R} + \frac{1}{2}\frac{r}{R}\sqrt{\frac{R^2 - r^2}{R^2}} \right) \right] \\ L' &= \frac{\mu_0 r}{2} \left(\ln\left(\frac{8r}{j}\right) - 2 \right) + \frac{\mu_0 r}{2} \left(\ln\left(\frac{r}{j}\right) - 1 \right). \end{aligned} \tag{3}$$

In which, t_m is the thickness of the metallic layer, t_d is the thickness of the dielectric layer, μ is the permeability of the dielectric layer, μ_0 is the permeability of the medium, and j is the radius of the area through which the current flows.

For each layer of the material structure, the inductance of the structural layer can be calculated using the following formula:

$$L_m = \frac{1}{\frac{2}{L} + \frac{1}{L'}}. \tag{4}$$

The resonant frequency is calculated using the following formula:

$$f = \frac{1}{2\pi\sqrt{L_m C_m}} \tag{5}$$

The values of inductance L, capacitance C, and resonant frequency f of the layers within the structure were calculated according to the aforementioned formulas. The values of (L,C) in Figures 9a, 9b, and 9c are specifically (L_1,C_1), (L_2,C_2), and (L_3,C_3), respectively.

For the first layer in Fig. 9a, the radii are given, resulting in a calculated resonant frequency of 5.78 THz. For the second layer in Fig. 9b, the radii are given, resulting in a calculated resonant frequency of 6.83 THz. For the third layer in Fig. 9c, the radii are given, resulting in a calculated resonant frequency of 7.68 THz.

These calculated results are consistent with experimental and simulation results and confirm the correctness of our circuit analysis.

3.4. Impedance

In order to provide a quantitative analysis of the operational principles of the proposed MMA. Based on our simulation, we obtained the coefficients S_{11}, S_{21}. The calculation of normalized impedance is performed based on the following formula:

$$Z(\omega) = \sqrt{\frac{(1+S_{11}(\omega))^2 - {S_{21}}^2(\omega)}{(1-S_{11}(\omega))^2 - {S_{21}}^2(\omega)}}. \tag{6}$$

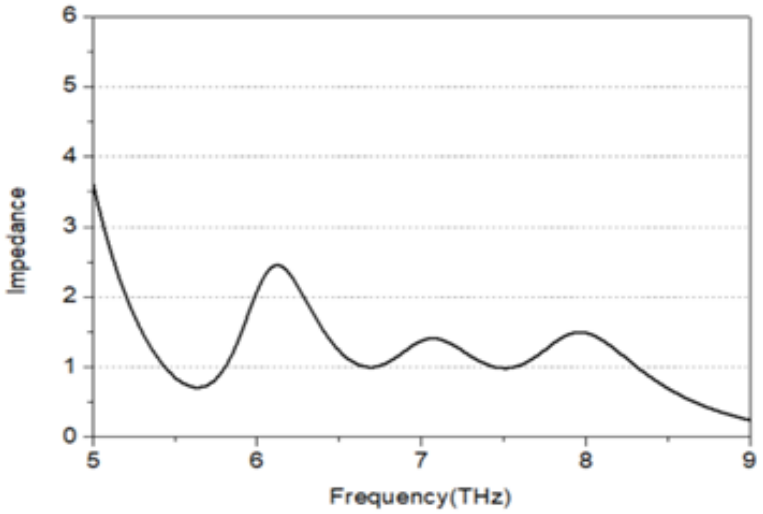

Fig. 11. Impedance of the optimal absorber structure and frequency.

From the results as presented in Fig. 11, it can be concluded that the impedance mismatch lies around a value close to 1, with errors occurring due to the method we used for calculation. This method overlooks the magnetic coupling response between the top structural layer and the bottom copper layer, leading to deviations from the actual intrinsic parameters. The conclusion is that this multilayer material exhibits good impedance matching with the surrounding environment, helping to clarify the material's absorption mechanism capability.

4. Conclusion

This study has conducted the design, simulation, and optimization of a broadband metamaterial absorber with a multilayer disk structure. Through the process of combining various materials and adjusting the correlation parameters between them, the optimal three-layer structure demonstrates a high absorption capability within the frequency range of 5.6-7.9 THz, with an average absorption rate of up to 90%. The analytical results regarding the distribution of electric and magnetic fields on the surface of the material as well as the current and equivalent circuit model provide deeper insights into the absorption principles of the structure. Notably, this structure also demonstrates an advantage in its ability to function effectively when the angle of incidence of the wave is altered up to over 45 degrees. The study shows that there are many prospects for such metamaterial absorbers in the fields of modern THz applications.

Acknowledgment

This research is funded by Vietnam National Foundation for Science and Technology Development (NAFOSTED) under grant number 103.02-2021.120.

Conflict of interest

The authors have no conflict of interest to declare.

References

[1] R. Kumar, M. Kumar, J. S. Chohan and S. Kumar, *Overview on metamaterial: History, types and applications*, Mater. Today: Proc. **56** (2022) 3016.

[2] M. K. Hedayati, F. Faupel and M. Elbahri, *Review of plasmonic nanocomposite metamaterial absorber*, Materials **7** (2014) 1221.

[3] J. Y. Rhee, Y. J. Yoo, K. W. Kim, Y. J. Kim and Y. P. Lee, *Metamaterial-based perfect absorbers*, J. Electromagn. Waves Appl. **28** (2014) 1541.

[4] M. E. H. Bakir, M. Karaaslan, O. Akgol, O. Altintas, E. Unal and C. Sabah, *Sensory applications of resonator based metamaterial absorber*, Optik **168** (2018) 741.

[5] M. Berka, H. A. Azzeddine, A. Bendaoudi, Z. Mahdjoub and A. Y. Rouabhi, *Dual-band bandpass filter based on electromagnetic coupling of twin square metamaterial resonators (srrs) and complementary resonator (csrr) for wireless communications*, J. Electron. Mater. **50** (2021) 4887.

[6] S. Mahfooz, A. Wakeel, M. Sibghat Ullah, M. Alam, A. Masood Siddiqui and A. Iftikhar, *A novel, mutual coupling independent, ultra-thin, and polarization-insensitive tetra band metamaterial absorber for microwave applications*, Waves Random Complex Media (2024) 1.

[7] Z. Zhan, Y. Han and Y. Zhang, *Rapid design of broadband absorption metasurfaces for selective tailoring of infrared radiation characteristics*, J. Phys. D: Appl. Phys. **54** (2021) 415102.

[8] M. Zhang and Z. Song, *Switchable terahertz metamaterial absorber with broadband absorption and multiband absorption*, Opt. Express **29** (2021) 21551.

[9] P. Fu, *A broadband metamaterial absorber based on multi-layer graphene in the terahertz region*, Opt. Commun. **417** (2018) 62.
[10] D. Pham-Van, C. Tran-Manh, N. Bui-Huu, A. Pham-Phuong, T. Ta-Minh-Tuan, D. Pham-Hoang *et al.*, *Broadband microwave coding absorber using genetic algorithm*, Opt. Mater. **147** (2024) 114679.
[11] M. C. Tran, V. H. Pham, T. H. Ho, T. T. Nguyen, H. T. Do, X. K. Bui *et al.*, *Broadband microwave coding metamaterial absorbers*, Sci. Rep. **10** (2020) 1810.
[12] C. Du, D. Zhou, H.-H. Guo, Y.-Q. Pang, H.-Y. Shi, W.-F. Liu *et al.*, *An ultra-broadband terahertz metamaterial coherent absorber using multilayer electric ring resonator structures based on anti-reflection coating*, Nanoscale **12** (2020) 9769.
[13] Y. Sun, Y. Shi, X. Liu, J. Song, M. Li, X. Wang *et al.*, *A wide-angle and te/tm polarization-insensitive terahertz metamaterial near-perfect absorber based on a multi-layer plasmonic structure*, Nanoscale Adv. **3** (2021) 4072.
[14] P. Yu, L. V. Besteiro, Y. Huang, J. Wu, L. Fu, H. H. Tan *et al.*, *Broadband metamaterial absorbers*, Adv. Opt. Mater. **7** (2019) 1800995.
[15] Y. Zhou, Z. Qin, Z. Liang, D. Meng, H. Xu, D. R. Smith *et al.*, *Ultra-broadband metamaterial absorbers from long to very long infrared regimes*, Light: Sci. Appl. **10** (2021) 138.
[16] Y. Kim, Y. J. Yoo, K. W. Kim, J. Y. Rhee, Y. H. Kim and Y. Lee, *Dual broadband metamaterial absorber*, Opt. Express **23** (2015) 3861.
[17] B. X. Khuyen, N. N. Viet, P. T. Son, B. H. Nguyen, N. H. Anh, D. T. Chi *et al.*, *Multi-layered metamaterial absorber: Electromagnetic and thermal characterization*, Photonics **11** (2024) 219.
[18] D. T. Ha, B. S. Tung, B. X. Khuyen, T. S. Pham, N. T. Tung and N. H. Tung, *Dual-band, polarization-insensitive, ultrathin and flexible metamaterial absorber based on high-order magnetic resonance*, Photonics **8** (2021) .
[19] D. Q. Vu, D. H. Le, H. T. Dinh, T. G. Trinh, L. Yue, D. T. Le *et al.*, *Broadening the absorption bandwidth of metamaterial absorber by coupling three dipole resonances*, Physica B: Condens. Matter **532** (2018) 90.
[20] M. Bağmancĭ, *Broadband multi-layered stepped cone shaped metamaterial absorber for energy harvesting and stealth applications*, Eng. Rep. (2024) e12903.